Nonlinear Dynamics and Neuroscience

Izvestiya Vysshikh Uchebnykh Zavedeniy. Applied Nonlinear Dynamics. 2025;33(4)

Article DOI: 10.18500/0869-6632-003175

Investigation of wave processes and rhythmic activity of the human brain using the Walsh orthogonal function system

I. V. Stepanyan✉, *M. Y. Lednev*

Mechanical Engineering Research Institute of the RAS, Moscow, Russia
E-mail: ✉neurocomp.pro@gmail.com, miklesus@mail.ru
Received 8.10.2024, accepted 24.02.2025, available online 22.04.2025, published 31.07.2025

Abstract. The *purpose* of this work is to study the wave processes and rhythmic activity of the brain based on multiscale parametric maps of electroencephalograms obtained as a result of algorithmic application of a system of discrete functions. *Methods.* For visualization, a previously developed multi-scale method for constructing parametric mappings of molecular genetic information was used, in which a set of four nucleotides is considered as a system of orthogonal Walsh functions. *Results.* The article proposes a new method of visualization of electroencephalography data for the study of rhythmic and wave processes of bioelectric activity of the brain. To analyze the electroencephalography data, the stage of transcoding the recorded amplitudes was previously carried out by one-to-one conversion of the EEG signal into a symbolic sequence, the alphabet of which consisted of four characters. Based on this method, the EEG signals of the subject were compared at rest and under mental stress. The study analyzed the readings of electrodes registering biopotentials of the frontal lobes of the brain. *Conclusion.* New methods have made it possible to identify various configurations of clusters in the frequency space of visualization, which can be used for comparative analysis of encephalograms and identification of features of recorded EEG signals. Specialized software has been developed as a tool for studying the rhythmic activity of the brain by constructing parametric displays of electroencephalograms.

Keywords: visualization algorithms, EEG, biopotentials, orthogonal function system, software, cluster analysis.

Acknowledgements. The work was performed within the framework of the State Assignment, code of scientific topic FFGU-2024-0019.

For citation: Stepanyan IV, Lednev MY. Investigation of wave processes and rhythmic activity of the human brain using the Walsh orthogonal function system. Izvestiya VUZ. Applied Nonlinear Dynamics. 2025;33(4):545–556. DOI: 10.18500/0869-6632-003175

Introduction

Encephalography is a method for studying the functional state of the human cerebral cortex by measuring its electrical activity [1]. A multichannel encephalograph records signals from the combined electrical activity of groups of nerve cells, consisting of millions of neurons and interneuronal synaptic connections. Thus, encephalography allows for the study of wave processes associated with various types of rhythmic brain activity. An electroencephalogram (EEG) contains a noise signal with a characteristic frequency spectrum depending on the encephalograph lead and the subject's state. These frequencies are calculated using the Fourier transform. Recently, a growing number of publications have explored the use of the Walsh-Hadamard transform, wavelet analysis methods, and machine learning for analyzing EEG data [2–9].

There are also known works on the development of new methods and tools for visualizing electroencephalography data [10–21].

We previously developed molecular genetic algorithms based on a system of orthogonal Walsh functions for multi-scale visualization of DNA parameters, taking into account the physicochemical structure of nucleotides. Our research [22, 23] revealed that molecular genetic algorithms can be applied to the analysis of long symbolic or numeric sequences reduced to tetra-representation, that is, recoded so that these sequences consist of four symbols, analogous to the four DNA nucleotides. We found that the developed visualization algorithms can reveal hidden cycles in long sequences. This was demonstrated in our work [22], where we analyzed various noise generators. It was shown that pseudorandom noise generators (i.e., those containing hidden periodicity) exhibit pronounced symmetry in two-dimensional visualization. At the same time, noise generators without internal cycles produced chaotic two-dimensional displays when applied to the new visualization algorithms. Hidden cycles are also clearly visible in one-dimensional displays.

The purpose of this work is to test the application of the Walsh orthogonal function system (which was previously used by the authors in molecular genetic algorithms) for visualization and analysis of human brain biopotentials obtained as a result of electroencephalographic studies.

1. Methodology

All reasoning is performed in accordance with previously developed methods described in [22, 23]. To analyze the EEG data, the amplitude information was recoded into a quaternary representation consisting of the symbols A, G, T, and C. Let us recall the main ideas of the basic algorithm, which consists of three steps.

1. **Scaling**. The sequence of symbolic elements of the set {A, G, C, T} encoding the analyzed signal is divided into fragments of equal length N with a given overlap step. The overlap step and the length N are free parameters of the algorithm and are responsible for the clarity and scale of the representations, respectively. The resulting fragments will henceforth be referred to as N-measures.
2. **Parameterization**. Given the Walsh function system defining genetic subalphabets, according to which each nucleotide has three binary representations (purine/primidine, keto/amino, 2/3 hydrogen bonds), the sequence of nitrogenous bases receives three binary representations. Together with the presence of a phosphate residue (which is not opposing, as it is present in all nucleotides), the three binary-opposing representations, which are taken into account during the parameterization stage, define the Walsh function system. For more details, see [1, 2].
3. **Display**. The final mapping is constructed from the three resulting N-dimensional sequences. It should be noted that mappings can be constructed in various coordinate systems, including polar, spherical, cylindrical, and others. This requires further research, taking into account the ergonomics of perception and the specifics of the data being analyzed. Depending on the number of binary sub-alphabets, one-dimensional, two-dimensional, and three-dimensional projections are possible. The following options have been developed for constructing mappings:
   (a) *structural visualization spaces* — display decimal representations of N-mers;
   (b) *frequency visualization spaces* — display relative or absolute frequencies of N-mers;
   (c) *integral visualization spaces* — display the number of specific symbols in each N-mer as

numerical indices in binary sub-alphabetic representations of the N-mers.

To apply visualization algorithms to encephalography tasks, the source data for analysis were taken from the resource PhysioNet [20]. According to the description of the experiment given in [21], among other parameters, the following is specified: «the sampling frequency was 500 Hz per channel. A high-pass filter with a cutoff frequency of 0.5 Hz, a low-pass filter with a cutoff frequency of 45 Hz, and a band-pass filter (50 Hz)». Recordings were carried out in two states of the subject: rest and under mental stress in the form of performing arithmetic calculations in his head. The study took into account readings from two electrodes: Fp1 and Fp2 (Fig. 1, 2). Description of the equipment and method of EEG recording is given in [21].

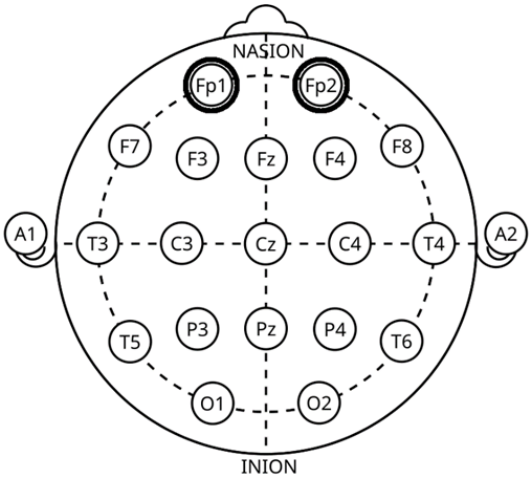

Fig. 1. Schematic arrangement of the electrodes. The electrodes are marked, the recordings from which were considered in this study

The study's hypothesis is that molecular genetic algorithms based on Walsh functions will enable the mapping of boundary states between strict cycles and chaotic components in EEG (i.e., between perfectly symmetric and chaotic two-dimensional representations). The EEG signal samples were recoded as follows. The original real values were converted to integers in the range $[0; 65535]$, which equals 16 bits per sample. In this case, no losses occur, as the characteristics of the processed signal specify that 16 bits are also allocated for real values. Next, each sample was converted to binary notation, and pairs of non-overlapping bits were converted to the corresponding symbol according to the following rule:

$$00_2 \to A, 01_2 \to C, 10_2 \to G, 11_2 \to T.$$

For example, for the number 26481 the encoding process looks like this:

$$26481_{10} \to 0110011101110001_2 \to (01)(10)(01)(11)(01)(11)(00)(01) \to CGCTCTAC.$$

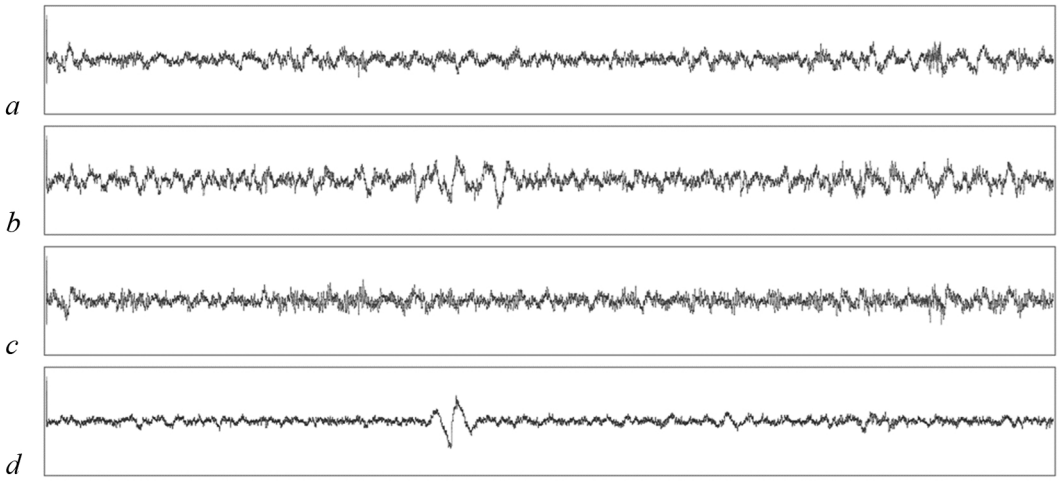

Fig. 2. Initial EEG signals. *a* — Fp1 electrode, resting state; *b* — electrode Fp1, mental load; *c* — electrode Fp2, resting state; *d* — Fp2 electrode, mental load

Each sample after encoding corresponds to 8 symbols. Therefore, the visualization scale should also be a multiple of 8. For structural displays, a scale of 16 was chosen to further separate the points on the plane (each point encodes a pair of samples). When calculating the frequency characteristics of each individual sample and constructing frequency visualizations, a scale of 8 was chosen. For structural and frequency displays, the step is equal to the scale because otherwise, the resulting values would consist of parts of the symbolic representation of adjacent reports. For integral displays, a step of one was chosen to increase the point density (with a step of one, the values are visually connected, forming a continuous curve). All this increased the information content and clarity of the resulting visualizations.

2. Results

Comparative analysis of human functional states based on EEG visualization data using the Walsh function system. As a result of the conducted study, binary-orthogonal mappings of EEG signals were constructed in various visualization spaces (Fig. 3, 4. 5). Chaotic and wave processes can be observed in the one-dimensional mappings shown in Fig. 3, where the *a*–*d* series are chaotic in nature, and the *e*–*f* series are wave-like. It should be noted that integral mappings are generally convenient for analyzing hidden wave processes. As can be seen from the first column in Fig. 4, two-dimensional structural mappings, in the presence of clear structuring, have a pronounced chaotic component, which confirms the possibility of visualizing a combination of ordered and noise components of EEG signals in a single parametric mapping.

At the same time, in the third column of Fig. 4, the integral maps exhibit virtually no symmetries, indicating the presence of a significant chaotic component (exact symmetries in

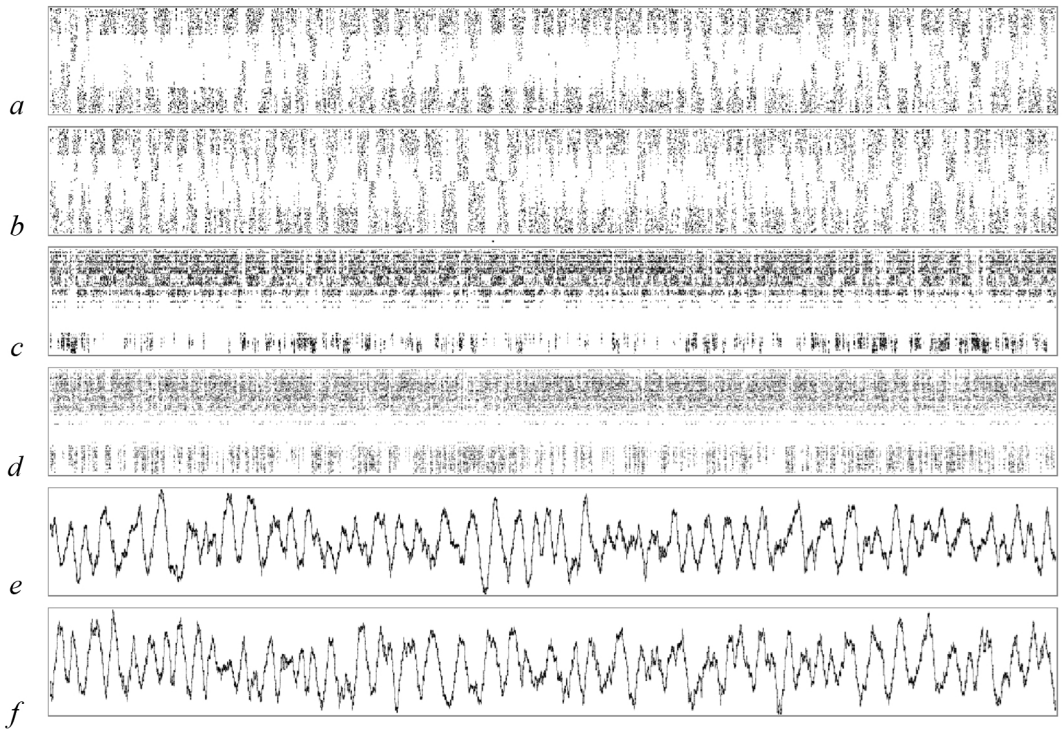

Fig. 3. One-dimensional mappings according to the purine-pyrimidine sub-alphabet of records from the Fp1 sensor. The resting state is shown in Figures *a*, *c*, *e*; the test for performing arithmetic calculations in mind is shown in Figures *b*, *d*, *f*. *a*, *b* — structural mappings at scale $N = 16$ and step 16; *c*, *d* are frequency mappings at scale $N = 8$ and step 8; *e*, *f* are integral mappings at scale $N = 1600$ and step 1

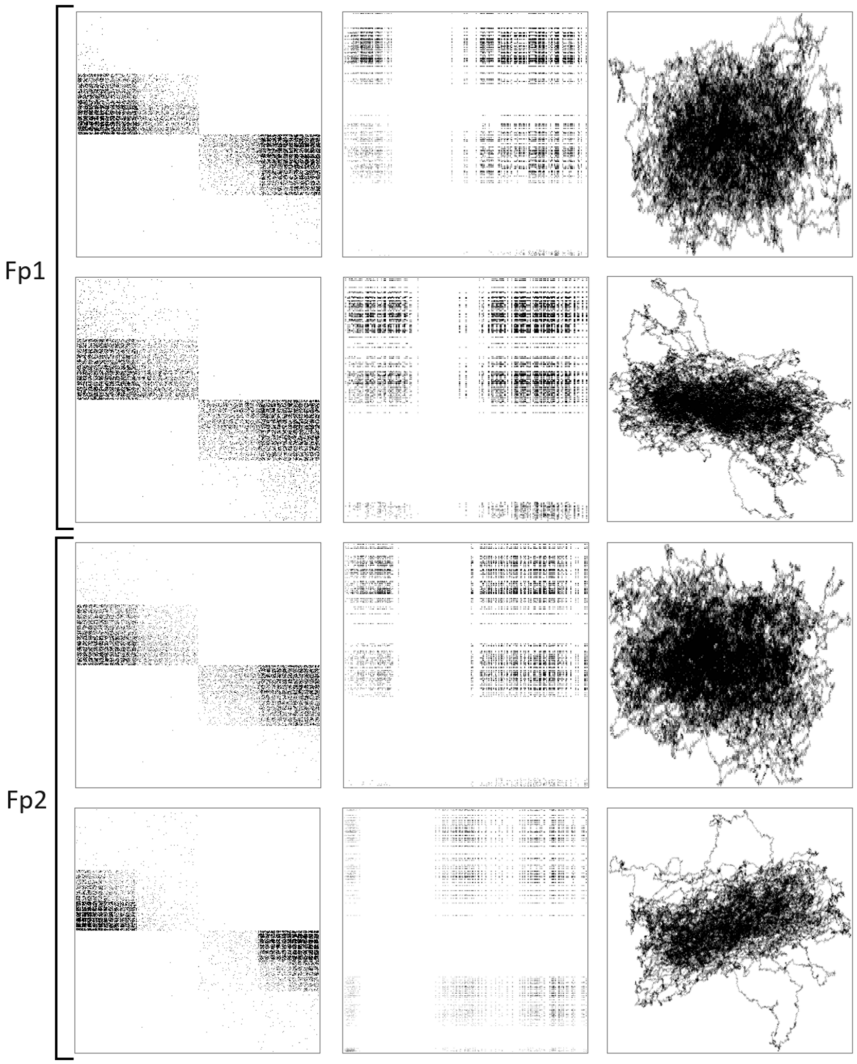

Fig. 4. Two-dimensional maps by the purine-pyrimidine (X) and keto-amino (Y) sub–alphabets. The first column is the structural maps at scale $N = 16$ and step 16. The second column is the frequency mappings at scale $N = 8$ and step 8. The third column is the integral mappings at scale $N = 1600$ and step 1. The first and third rows are the state of rest, the second and fourth rows are the mental load

these maps can be observed in repeating signals, for example, in long pseudorandom sequences). During experiments with various EEG signals, we observed that the characteristic "tangle"shapes of the integral two-dimensional representations varied greatly among different EEG signals and sometimes took the form of double formations (Fig. 5).

The application of the proposed visualization method allows us to obtain new characteristics of EEG signals in the form of a structure of three-dimensional clusters in the frequency space of visualization: mutual arrangement, shape and number of clusters (in Fig. 6 some different clusters are highlighted with a frame).

Fig. 6 clearly shows the differences in the structure and number of frequency clusters in the encephalographic signals obtained from various EEG leads during and without mental stress. As can be seen from the figure, the cluster structure of the displays differs significantly across the subject's different functional states. It is evident that additional frequency clusters are formed during mental stress. These clusters are designated in the figure as σ_1 and σ_2 and require further

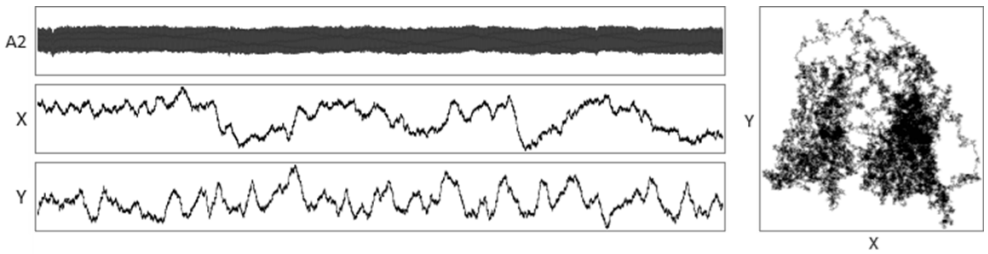

Fig. 5. Example of integral EEG signal mappings at $N = 1600$ and overlap step 1. The first column shows the curves of the initial signal with the designation of the electrode and one-dimensional maps by sub-alphabets: keto-amino (X); 2 or 3 hydrogen bonds (Y). The second column shows a two-dimensional integral mapping according to the corresponding sub-alphabets

study.

Fig. 7 shows some examples of binary orthogonal displays of EEG signals in various visualization spaces. The visualization of the EEG recording is shown in one-dimensional (top row), two-dimensional (middle row), and three-dimensional (bottom row) representations. For convenience, the original signal is presented above each display type (structural, frequency, and integral).

It's logical to assume that conversion to other number systems (not only quaternary, but also quinary, sexagenary, and others) allows for the application of similar methods. Hadamard matrices of various orders exist, encoding various systems of Walsh orthogonal functions. A useful property of the matrices that describe nucleotide encoding, which were used in this study, is that they allow for the construction of visualizations in three-dimensional space. This is clear and easy to understand. Matrices of higher order yield more dimensions, and various two-dimensional and three-dimensional projections of multidimensional visualization spaces can be considered. Thus, the proposed mathematical framework suggests further research.

Methods are known for visualizing dynamics from a one-dimensional data set (in particular,

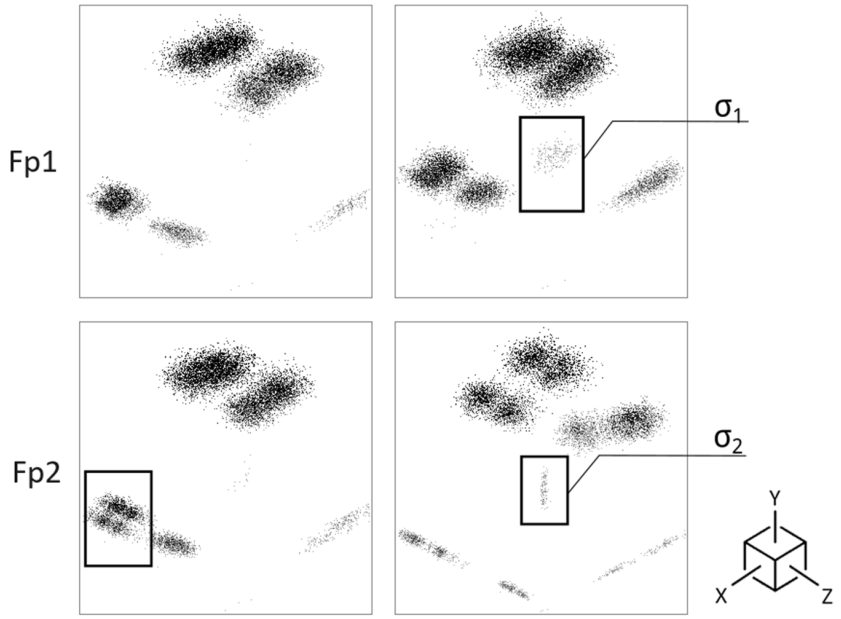

Fig. 6. Three-dimensional frequency maps at scale $N = 8$ and step 8 for the purine-pyrimidine (X), 2 or 3 hydrogen bonds (Y) and keto–amino (Z) subalphabytes. The first column is the resting state, the second column is the mental load

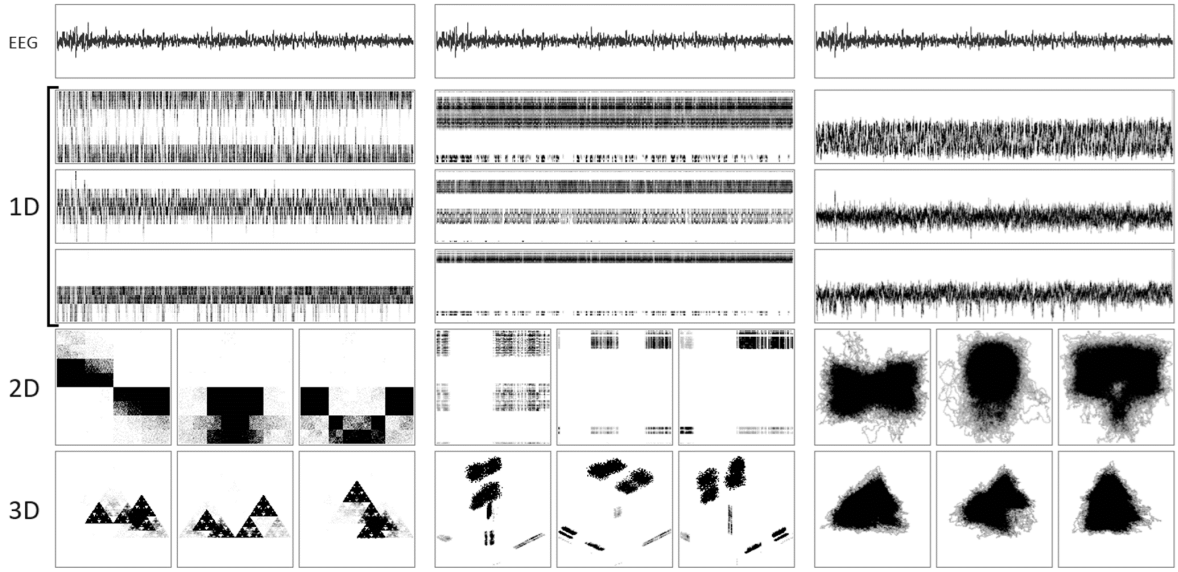

Fig. 7. Output of the encephalogram analysis program. The first column shows the structural visualization space at scale N=16 and overlap step 1. The second column shows the frequency space of visualizations at scale $N = 8$ and overlap step 8. The third column shows the integral visualization space at scale $N = 1600$ and overlap step 1. One-dimensional projections are displayed in sub-alphabets (from top to bottom): purine-pyrimidine (X), keto-amino (Y) and 2 or 3 hydrogen bonds (Z). Two-dimensional projections are presented in the following order (from left to right): XY, YZ, XZ. Three-dimensional projections: XYZ, XYZ, XYZ

using Takens' theorem). When visualizing in three-dimensional frequency space using the proposed method (for $N = 8$), the points are not related to their relative positions in the original signal. Furthermore, using a system of subalphabets in the Hadamard matrix allows for the application of Takens' theorem to each dimension separately. Thus, the proposed method complements nonlinear dynamics methods.

Conclusion

The conducted studies confirmed the feasibility of visualizing and comparing encephalograms recorded in various functional states of subjects using developed molecular genetic algorithms. The proposed method enables the display of parametric characteristics of EEG signals at various scales and in various visualization spaces through the specific application of Walsh functions. One of the most significant results of the study is the three-dimensional frequency clustering of EEG signals, which revealed a frequency cluster in both frontal lobes of the brain presumably responsible for the subject's mental workload.

The results of this study correlate with previously obtained data on the use of a system of Walsh functions to identify hidden cyclic structures in arbitrary signals [22]. We previously demonstrated in [24] that the use of a graph-theoretical approach allows us to calculate the quantitative characteristics of cyclic structures in EEG signals at various scales, as well as to calculate the indices of the EEG characteristic graph—the Euler number, the number of simple cycles, and the number of simple pathways. This study confirms the presence of hidden structures and a special kind of order in the recorded biopotentials of the human brain.

The study results were obtained using our own encephalogram analysis program, based on previously developed molecular genetic algorithms. The program, written in C++, enables real-time processing of EEG signals.

References

1. Ke J, Du J, Luo X. The effect of noise content and level on cognitive performance measured by electroencephalography (EEG). Automation in Construction. 2021;130:103836. DOI: 10.1016/j.autcon.2021.103836.
2. Prasanna JP, Subathra MSP, Mohammed MA, Maashi MS, Garcia-Zapirain B, Sairamya NJ, George ST. Detection of focal and non-focal electroencephalogram signals using fast Walsh-Hadamard transform and artificial neural network. Sensors. 2020;20(17):4952. DOI: 10.3390/s20174952.
3. Göker H, Tosun M. Fast Walsh–Hadamard transform and deep learning approach for diagnosing psychiatric diseases from electroencephalography (EEG) signals. Neural Comput. and Applic. 2023;35(32):23617–23630. DOI: 10.1007/s00521-023-08971-6.
4. Goshvarpour A, Goshvarpour A. Analytic representation vs. angle modulation of Hilbert transform of fast Walsh-Hadamard coefficients (HTFWHC) in epileptic EEG classification. Braz. J. Phys. 2023;53:15. DOI: 10.1007/s13538-022-01231-3.
5. Mohsen S, Ghoneim SSM, Alzaidi MS, Alzahrani A, Ali Hassan AM. Classification of electroencephalogram signals using LSTM and SVM based on fast walsh-hadamard transform. Comput. Mater. Contin. 2023;75(3):5271–5286. DOI: 10.32604/cmc.2023.038758.
6. Shakya N, Dubey R, Shrivastava L. Stress detection using EEG signal based on fast Walsh–Hadamard transform and voting classifier. Research Square. 2021. DOI: 10.21203/rs.3.rs-782483/v1.
7. Ergün E, Aydemir O. A hybrid BCI using singular value decomposition values of the fast Walsh–Hadamard transform coefficients. IEEE Transactions on Cognitive and Developmental Systems. 2020;15(2):454–463. DOI: 10.1109/TCDS.2020.3028785.
8. Yuan X, Cai Z. A generalized Walsh system and its fast algorithm. IEEE Transactions on Signal Processing. 2021;69:5222–5233. DOI: 10.1109/TSP.2021.3099635.
9. Widdess-Walsh P. Resting But Not Idle: Insights Into Epilepsy Network Suppression From Intracranial EEG. Epilepsy Currents. 2024;24(1):25–27. DOI: 10.1177/15357597231213247.
10. Vaithialingam B, Rudrappa S. Intraoperative visualisation of 3 Hz spike-wave epileptic discharges in the electroencephalographic signal of bispectral index monitor in a patient with absence seizures. Indian J. Anaesth. 2024;68(2):209–210. DOI: 10.4103/ija.ija_710_23.
11. Salami A, Andreu-Perez J, Gillmeister H. Finding neural correlates of depersonalisation/derealisation disorder via explainable CNN-based analysis guided by clinical assessment scores. Artif. Intell. Med.. 2024;149:102755. DOI: 10.1016/j.artmed.2023.102755.
12. Taylor JA, Garrido MI. Porthole and Stormcloud: tools for visualisation of spatiotemporal M/EEG statistics. Neuroinformatics. 2020;18(3):351–363. DOI: 10.1007/s12021-019-09447-6.
13. QiHan PW, Alipal J, Suberi AAM, Fuad N, Wahab MHA, Idrus SZS. A new perspective on visualising EEG signal of post-stroke patients. IOP Conf. Ser.: Mater. Sci. Eng. 2020;917(1):012047. DOI: 10.1088/1757-899X/917/1/012047.
14. Gómez LC, Hervás R, González I, Villarreal V. Studying the generalisability of cognitive load measured with EEG. Biomedical Signal Processing and Control. 2021;70:103032. DOI: 10.1016/j.bspc.2021.103032.
15. Caillet B, Devènes S, Maître G, Hight D, Mirra A, Levionnois O, Simalatsar A. General Anaesthesia Matlab-based Graphical User Interface: A tool for EEG signal acquisition, processing and visualisation offline and in real-time. 2023. DOI: 10.13140/RG.2.2.33243.68647.
16. Cao J, Zhao Y, Shan X, Wei HL, Guo Y, Chen L, Erkoyuncu JA, Sarrigiannis PG. Brain functional and effective connectivity based on electroencephalography recordings: A review. Hum. Brain Mapp. 2022;43(2):860–879. DOI: 10.1002/hbm.25683.

17. Cabañero L, Hervás R, González I, Fontecha J, Mondéjar T, Bravo J. Characterisation of mobile-device tasks by their associated cognitive load through EEG data processing. Future Generation Computer Systems. 2020;113:380–390. DOI: 10.1016/j.future.2020.07.013.
18. Costadopoulos N, Islam MZ, Tien D. A knowledge discovery and visualisation method for unearthing emotional states from physiological data. Int. J. Mach. Learn. & Cyber. 2021;12(3): 843–858. DOI: 10.1007/s13042-020-01205-4.
19. Montazeri S, Pinchefsky E, Tse I, Marchi V, Kohonen J, Kauppila M, Airaksinen M, Tapani K, Nevalainen P, Hahn C, Tam EWY, Stevenson NJ, Vanhatalo S. Building an open source classifier for the neonatal EEG background: a systematic feature-based approach from expert scoring to clinical visualization. Front. Hum. Neurosci. 2021;15:675154. DOI: 10.3389/fnhum.2021.675154.
20. Goldberger AL, Amaral LA, Glass L, Hausdorff JM, Ivanov PC, Mark RG, Mietus JE, Moody GB, Peng CK, Stanley HE. PhysioBank, PhysioToolkit, and PhysioNet: components of a new research resource for complex physiologic signals. Circulation. 2000;101(23):E215-220. DOI: 10.1161/01.cir.101.23.e215.
21. Zym I, Tukaev S, Seleznov I, Kiyono K, Popov A, Chernykh M, Shpenkov O. Electroencephalograms during Mental Arithmetic Task Performance. Data. 2019;4(1):14. DOI: 10.3390/data4010014.
22. Stepanyan IV, Lednev MY. Visualization of the Signals Entropy Structure Based on Walsh–Hadamard Functions. Symmetry. 2024;16(1):59.
23. Stepanyan IV, Lednev MY. Algorithms for visualization of molecular genetic sequences in spaces of binary-orthogonal Walsh functions. M.: "KDU", "Dobrosvet"; 2020. 193 p. (in Russian). DOI: 10.31453/kdu.ru.978-5-7913-1159-7-2020-193.
24. Aristov VV, Kubryak OV, Stepanyan IV. Calculation of cyclic characteristics of an electroencephalogram for the study of electrical activity of the brain. Izvestiya VUZ. Applied Nonlinear Dynamics. 2023;31(4):469–483 (in Russian). DOI: 10.18500/0869-6632-003051.